Identification of microRNA transcriptome throughout the lifespan of yak (*Bos grunniens*) corpus luteum

Shi Yin, Jingwen Zhou, Liuqing Yang, Yujie Yuan, Xianrong Xiong, Daoliang Lan & Jian Li

Taylor & Francis
Taylor & Francis Group

Check for updates

Identification of microRNA transcriptome throughout the lifespan of yak (*Bos grunniens*) corpus luteum

Shi Yin[a,b,c] (iD), Jingwen Zhou[a], Liuqing Yang[a,b], Yujie Yuan[a], Xianrong Xiong[a,b], Daoliang Lan[a,b], and Jian Li[a,b]

[a]Key Laboratory of Qinghai-Tibetan Plateau Animal Genetic Resource Reservation and Utilization, Qinghai-Tibetan Plateau Animal Genetic Resource Reservation and Utilization Key Laboratory of Sichuan Province, Ministry of Education, Southwest Minzu University, Chengdu, Sichuan, China; [b]College of Animal & Veterinary, Southwest Minzu University, Chengdu, Sichuan, China; [c]Key Laboratory of Modern Biotechnology, State Ethnic Affairs Commission, Southwest Minzu University, Chengdu, Sichuan, China

ABSTRACT

The corpus luteum (CL) is a temporary organ that plays a critical role for female fertility by maintaining the estrous cycle. MicroRNA (miRNA) is a class of non-coding RNAs involved in various biological processes. However, there exists limited knowledge of the role of miRNA in yak CL. In this study, we used high-throughput sequencing to study the transcriptome dynamics of miRNA in yak early (eCL), middle (mCL) and late-stage CL (lCL). A total of 6,730 miRNAs were identified, including 5,766 known and 964 novels miRNAs. Three miRNAs, including bta-miR-126-3p, bta-miR-143 and bta-miR-148a, exhibited the highest expressions in yak CLs of all the three stages. Most of the miRNAs were 20–24 nt in length and the peak was at 22 nt. Besides, most miRNAs with different lengths displayed significant uracil preference at the 5'-end. Furthermore, 1,067, 280 and 112 differentially expressed (DE) miRNAs were found in eCL vs. mCL, mCL vs. lCL, and eCL vs. lCL, respectively. Most of the DE miRNAs were down-regulated in the eCL vs. mCL and eCL vs. lCL groups, and up-regulated in the mCL vs. lCL group. A total of 18,904 target genes were identified, with 18,843 annotated. Pathway enrichment analysis of the DE miRNAs target genes illustrated that the most enriched cellular process in each group included pathways in cancer, PI3K-Akt pathway, endocytosis, and focal adhesion. A total of 20 putative target genes in 47 DE miRNAs were identified to be closely associated with the formation, function or regression of CL. Three DE miRNAs, including bta-miR-11972, novel-miR-619 and novel-miR-153, were proved to directly bind to the 3'-UTR of their predicated target mRNAs, including *CDK4*, *HSD17B1* and *MAP1LC3C*, respectively. Both of these DE miRNAs and their target mRNAs exhibited dynamic expression profiles across the lifespan of yak CL. This study presents a general basis for understanding of the regulation of miRNA on yak CL and also provides a novel genetic resource for future analysis of the gene network during the estrous cycle in the yak.

Introduction

The corpus luteum (CL) is a transient endocrine gland that is formed from an ovulated follicle. The normal formation, function and regression of CL are critical for the secretion of steroid hormone and the maintenance of intrauterine pregnancy.[1,2] Luteal cells are usually transformed from ovarian granulosa cells (GCs) luteinize into luteal cells after ovulation and following the activation of luteinizing hormone receptor (LH-R) and this event is referred as luteinization.[3] Besides, the development of the CL also involves several other

events such as endothelial cell migration, extracellular matrix (ECM) remolding and vascularization. Developing endothelial cells and vessels are observed in the early stage of CL.[3,4] In the middle luteal phase, concentrations of several hormones that are necessary for reproductive regulation, including progesterone, estradiol, and androstenedione, are reported to reach their peaks.[4–6] Among these hormones, progesterone is the most important as it plays a vital role in the regulation of the estrous cycle and maintaining pregnancy.[7,8] CL regression is also essential for normal reproductive function. The failure of CL degeneration

on schedule results in persistent progesterone secretion, follicular development inhibition, estrous cycle termination and infertility.[9,10] Several factors, such as autophagy, apoptosis, and cytokines are involved in the regulation of CL regression.[11–13] Compared with the early stage, mature endothelial cells, accumulating extracellular matrix fibers, and stabilized vessels are observed in the middle and late stage of CL. Besides, the late stage of CL contains circular regression areas, since the luteal cells are shrunken and scattered around the capillaries in this stage.[14] The dynamic changes that occur during CL development make it an ideal tissue for the study of diverse biological processes, such as cell proliferation, vasculogenesis, cellular matrix remodeling, steroidogenesis, and apoptosis.

Accompanied by drastic structural changes in transcriptional activity, various molecules participate in the regulation of CL. MicroRNA (miRNA) is a class of single-stranded nucleic acids between 18 and 25 nucleotides (nts) in length. miRNAs can regulate gene expression by base-pairing with complementary sequences in the 3′-untranslated region (UTR), 5′-UTR or coding region sequence of target mRNAs and result in targeted mRNAs degradation or translation inhibition.[15–18] The roles of miRNA in the CL have been widely studied in recent years. In female mice, mutations in the miRNA-processing enzyme DICER1 caused impaired CL angiogenesis and infertility. Further studies proved that two miRNAs, miR-17-5p and let-7b, were responsible for CL angiogenesis by repressing the expression of the anti-angiogenic factor tissue inhibitor of metalloproteinase 1 (Timp1).[19] In buffalo CLs, 3,018 miRNAs were identified and the predicted target genes were associated with various cellular house-keeping processes such as apoptosis.[20] A study on the miRNA transcriptome during the entire physiological estrous cycle in bovine CL revealed that 42 miRNAs were differentially expressed (DE) in the early stage of CL relative to other stages. Prediction analysis of DE miRNAs revealed that target genes involved in CL formation, maintenance and regression.[21] Another study identified 590 luteal miRNAs in the bovine CL during maternal recognition of pregnancy and the target genes of DE miRNAs involved in regulating apoptosis and immune response.[22] Furthermore, many miRNAs have been reported to be essential in the regulation of CL. In the mid-cycle of bovine luteal cells, increased concentrations of miR-34a resulted in decreased luteal cell proliferation and increased production of progesterone by repressing the expression of notch receptor 1 (Notch1) and YY1 transcription factor (YY1).[23] Another

miRNA, miR-29b, was found to promote progesterone secretion and proliferation of bovine CL cells via inhibition of oxytocin receptor (OXTR) expression.[24] In bovine luteal endothelial cells, miR-221 could inhibit the expression of Serpin Family E Member 1 (SERPINE1) and promote angiogenic characteristics of these cells.[25]

Yak is a unique animal husbandry species that lives on the Tibetan Plateau and has extremely important economic values. However, the yak usually has short estrus duration and low reproductive performance, which greatly restricts its production.[26,27] In recent years, numerous studies have reported the involvement of miRNAs in different organs of yak reproductive system, such as testis,[28] epididymis,[29] and ovary.[30,31] However, little is known about the involvement of miRNAs in yak CL even though it plays a vital role in the regulation of the estrous cycle. This study aimed to identify and analyze the miRNA transcriptome profile in yak CLs at different stages of the estrous cycle. The project we performed will provide a database for further functional analysis of miRNA in different stages of yak CL.

Materials and methods

Animals and tissue collection

Fresh ovaries from healthy non-pregnant female Maiwa yaks with similar body sizes and normal estrous cycles (3–5 years old) were collected from a slaughterhouse in Qingbaijiang Country, Chengdu, Sichuan Province. All the yaks were observed for behavioral signs of estrus and the day of standing heat was designated as day 0. The stage of the estrous cycle was further determined by assessing the color and consistency of the uterus and ovary as previously described.[32,33] Depending on the day of the estrous cycle and morphology, CLs were divided into early (eCL, day 3–4, 10–20 mm in diameter, red and rich in blood vessels), middle (mCL, day 10–11, 20–30 mm in diameter and pink with visible blood vessels on the outside) and late stages (lCL, day 15–16, 10–20 mm in diameter and was yellow-white with no visible blood vessels on the outside). Excess tissues around the ovary were removed and the CL was separated with RNase-free scissors. A total of nine CLs ($n = 3$ for each stage) were collected and each tissue was collected from individual animal. Each tissue was then divided into three pieces according to the needs for different experiments: one piece was fixed in 4% PFA for 24 hours at room temperature for paraffin-embedded tissue sections; one piece was cut into small

pieces of $1 \times 1 \times 0.5$ cm and placed in centrifuge tubes containing PBS (PH = 7.4) for progesterone detection; the rest of the tissue was cut into small pieces and placed in centrifuge tubes containing RNA laterTM (Invitrogen, AM7020) for RNA extraction. The tissues for progesterone detection and RNA extraction were then frozen rapidly in liquid nitrogen and stored at $-80\,^{\circ}$C. Sample collection was carried out under the license in accordance with the Guideline for Care and Use of Laboratory Animals of China and was performed following the permit guidelines established by Southwest Minzu University, China.

Histological analysis

Paraffin-embedded samples at different stages of yak CLs were cut into 5 μm sections. Hematoxylin staining were performed using a Hematoxylin-eosin staining kit (Solarbio G1120, Beijing, China) according to the manufacturer's instruction. Images of the stained samples were photographed by using an optical inverted microscope (Leica DMi1, Germany).

Progesterone detection

The tissues at different stages were thawed, homogenized and centrifuged at 3, 000 rpm/min for 20 min at $4\,^{\circ}$C. The supernatant was then collected and the concentration of progesterone was detected by Elisa using a Bovine PROG ELISA Kit (Ruixin, 72282) according to the manufacturer's instruction.

Library preparation for small RNA (sRNA) sequencing

Total RNA was extracted using Trizol (Invitrogen, 15596026), and agarose gel electrophoresis was performed to determine RNA integrity and eliminate DNA contamination. RNA purity (OD260/280 and OD260/230) was determined using a Nanophotometer Spectrometer (NanoDrop, ND-2000) and RNA concentration was quantified by QUBIT2.0 (Life Technologies). Library construction was performed under the guidance of a Small RNA Sample Pre Kit (Illumina, RS-200-0048). Briefly, the 3'SR and 5'SR adaptors were ligated and the first chain was subsequently synthesized by reverse transcription. After PCR amplification, target DNA fragments were separated by PAGE electrophoresis and the cDNA library was obtained after gel extraction. At last, PCR products were purified (AMPure XP system) and the

quality of sequenced samples was assessed by calculating probabilities of error for each base-call using *Phred*.[20]

Clustering, sequencing and quality control

Clustering of the index-coded samples was performed on a cBot Cluster Generation System using a TruSeq PE Cluster Kit v4-cBot-HS (Illumia) according to the manufacturer's instruction. Following cluster generation, the library preparations were sequenced on an Illumina platform and single-end reads were generated. Raw data (raw reads) of fastq format were processed through in-house perl scripts. In this step, clean data (clean reads) were obtained by removing the reads containing the adapter and ploy-N through cutadaptor (version: 1.91). Low-quality reads from raw data and reads shorter than 18 nt or longer than 30 nt were also trimmed. At the same time, the quality score (Q-score), GC-content, and sequence duplication level of the clean data were calculated. All the downstream analyses were based on clean data with high qualities.

Annotation of sRNAs and identification of miRNAs

The clean reads were aligned with Silva (https://www.arb-silva.de/), GtRNAdb (http://gtrnadb.ucsc.edu/), Rfam (http://rfam.xfam.org/) and Repbase database (https://www.girinst.org/repbase/), respectively, using the HISAT2 (version: 2.0.4) software. Ribosomal RNA (rRNA), transfer RNA (tRNA), small nuclear RNA (snRNA), small nucleolar RNA (snoRNA) and other ncRNA/repeats were filtered. Mapped reads were further obtained by comparing the unannotated reads with the reference genome (Bos_mutus. BosGru_v2.0) using HISAT2. Then the mapped reads were compared with the known miRNA mature sequence (containing the ranges between 2 nt upstream to 5 nt downstream) in the miRBase (v22) database and at most one mismatch was allowed. These reads were considered as known miRNAs. Novel miRNAs were predicated using miRDeep2 based on the structure and energy of precursor sequences.

Quantification of miRNA expression levels

miRNA expressions were normalized using the TPM Algorithm. Differential expression analysis was performed by applying the DESeq2 R package (1.10.1). p Values were adjusted by adopting the Benjamini and Hochberg's approach to control the false

discovery rate. miRNAs with |log2 (Fold Change) |$\geq$1.00 and p value $\leq$0.05 were considered to be differentially expressed.

Functional annotation of miRNA target gene

Gene function was annotated based on the following databases: Nr (ftp://ftp.ncbi.nlm.nih.gov/blast/db), Pfam (http://pfam.xfam.org/), KOG/COG (http://www.ncbi. nlm.nih.gov/COG/), Swiss-Prot (http://ftp.ebi.ac.uk/pub/ databases/swissprot) and KEGG (https://www.genome. jp/kegg).

Real-time PCR for miRNA quantitation

Total RNA was extracted using Trizol, and cDNA synthesis was performed using a miRNA First Strand cDNA Synthesis Kit (Tailing Reaction) (Sangon Biotech (Shanghai), B532451) based on the manufacturer's instruction. The reaction system was as follows: 10 μL 2 × miRNA RT Solution mix, 2 μL miRNA RT Enzyme mix, 2 μL RNA and 6 μL ddH$_2$O. The reaction was carried out at 37 °C for 60 min and 85 °C for 5 min. Real-time PCR was performed under the guidance of miRcute Plus miRNA qPCR Detection Kit (SYBR Green) (TIANGEN, FP401) and 20 μL of the following PCR reaction mix was added: 10 μL 2 × miRcute Plus miRNA Premix (with SYBR&ROX), 0.5 μL 10 μM primers (forward and reverse each), 1 μL cDNA, and 8 μL ddH$_2$O. PCR program consisted of 40 cycles of 95 °C for 15 min, 94 °C for 20 s, and 64 °C for 30 s. U6 was choosed as the reference gene for miRNA quantitation. The comparative C$_T$ method was used to calculate the fold change in gene expression. All PCR primers were listed in Table S1.

Real-time PCR for mRNA quantitation

cDNA was synthesized by applying a PrimeScript TM reagent Kit (Takara, RR047A, Osaka, Japan) according to the manufacturer's instruction. The Real-time PCR reaction mixture contained 5 μL Real-time PCR Master (Roche, 04913914001), 0.5 μL 10 μM primers (forward and reverse each), 1 μL cDNA, and 3 μL ddH$_2$O. PCR program was as follows: 95 °C for 3 min, 95 °C for 10 s, and 60 °C for 31 s. The second and third steps were repeated for 40 cycles. Considering that CL is a temporal gland and undergoes dramatic changes during the entire estrous cycle, data were normalized against two reference genes, CNOT11 and SUZ12, respectively, as these genes have been proven to be the optimal reference genes in the CL obtained from cyclic or pregnant cows.[34] The quantification of the fold change of gene expression was determined using the comparative C$_T$ method. PCR primers were listed in Table S1.

Luciferase reporter vector construction

The 3′-UTRs of yak CDK4, HSD17B1 and MAP1LC3C mRNAs that contains the putative miRNA binding sites were synthesized. These oligonucleotides were digested with NheI and XbaI and inserted into the pmirGLO luciferase reporter vector (GeneCreate Biotech) at the corresponding restriction sites. The sequences of inserted fragments were verified by sequencing.

Luciferase assay

HEK 293 T cell was transfected using Lipofectamine 2000 (Invitrogen, 11668-027) following the manufacturer's instruction. Briefly, 5×10^3 cells were plated in a 96-well tissue culture plate the day before transfection. For each group, 200 ng luciferase reporter vectors, together with 5pM miRNA mimics or negative control miRNAs (ReBoBio) were incubated with 0.25 μL Lipofectamine 2000 （Invitrogen, 11668-027） and transfected into cells. The solution was replaced with fresh medium after 4 hours and the cell lysates were collected 24hours after transfection. The luciferase activities were assayed using the Dual-Luciferase Reporter Assay System (Beyotime, RG027) according to the manufacturer's instruction.

Statistical analysis

Statistical analysis was performed using one-way ANOVA (Tukey's multiple comparison test). All experiments were carried out at least three times and the results were presented as mean ± SEM. Statistical significance was set at $p < 0.05$.

Results

Small RNA sequence quality assessment and miRNA identification in yak CLs

The stages of yak CL were assessed by histological examination and progesterone detection. Hematoxylin staining and progesterone detection showed that the eCL, mCL, and lCL displayed different histological structures and progesterone concentrations (Fig. S1). RNA quality was assessed using the RNA Integrity Number (RIN) and samples with RIN scores higher

Table 1. Evaluation of sequencing data.

Samples	RIN	Raw reads	Clean reads	GC (%)	Low quality	Containing 'N' reads	Length <18	Length >30	Q30 (%)
eCL1	7.9	17,746,308	12,707,726	50.96	0	0	515,198	4,523,384	96.70
eCL2	8.0	16,585,279	14,003,103	51.08	0	0	1,493,178	1,088,998	96.60
eCL3	8.5	18,088,506	16,487,673	49.28	0	0	669,415	931,418	96.86
mCL1	7.9	14,333,625	11,262,832	49.98	0	0	242,849	2,827,944	96.56
mCL2	7.8	16,880,238	15,461,667	49.46	0	0	439,280	979,291	96.80
mCL3	8.4	12,592,890	11,784,418	49.20	0	0	256,248	552,224	96.98
lCL1	8.3	18,270,173	16,258,404	49.29	0	0	314,813	1,696,956	96.74
lCL2	9.0	13,988,438	12,209,133	49.78	0	0	813,702	965,603	94.85
lCL3	7.8	13,171,794	12,170,597	49.26	0	0	531,746	469,451	97.07
Average	8.2	15,739,695	13,593,950	49.81	0	0	586,270	1,559,474	96.57

eCL1 to eCL3, mCL1 to mCL2 and lCL1 to lCL3 represented three replicate yak CL samples in early, middle and late stages, respectively. The same as below.
RIN: The RNA integrity number.
Clean reads: The number of reads with a Q-score of 30 or greater.
Low quality: The number of reads contains more than 20% bases with a Q-score <30.
Containing 'N' reads: The number of reads contains at least 10% of the unknown base N.
Q30: The percentage of base calls with a Q-score of 30 or greater.

than 6 were considered to be of high quality.[35] Here the RIN value of nine CL samples was between 7.8 and 9.0 (Table 1), which indicated that the qualities of these samples were suitable for library construction. The average raw data and clean data of the nine samples were $15,739,695 \pm 2,222,128$ (mean ± SD) and $13,593,950 \pm 2,017,618$ (mean ± SD), respectively. Q-score is a measure for sequencing accuracy. Base calls with an average quality Q-score of 30 or greater means the presence of one incorrect base call or less in 1,000 and therefore having an error probability ≤ 0.001.[36] High quality reads are considered to be more than 90% reads have an average Q-score $>=30$.[20] Here more than 94.5% of reads in each sample had a Q-score higher than 30 and the average Q-score of the nine samples was 96.57% (Table 1). These results indicated that the obtained data were of high quality.

Length distribution analysis showed that the length of the clean reads mainly ranged between 20 and 24 nt and the peak was at 22 nt (Fig. 1A), which was consistent with the reported length distribution of miRNA. sRNAs were annotated and classified by aligning clean reads with different databases. The proportions of unannotated reads containing miRNA were more than 80% in each sample (Fig. 1B). Mapped reads were obtained by comparing the unannotated reads with the reference genome. Totally, 6,730 miRNAs were obtained, of which 5,766 were known and 964 were predicted. mCL1 had the least number of miRNAs (5,347) and eCL3 had the highest number of miRNAs (6,239). The number of miRNAs in different samples were listed in Table S2 and the detailed information of each miRNA was displayed in Table S3.

The top ten most abundant miRNAs in each stage were listed (Fig. 1C–E). Notably, most of these miRNAs displayed higher expression levels across the entire estrous cycle. Three of them, bta-miR-126-3p, bta-miR-143 and bta-miR-148a, ranked first in eCL, mCL, and lCL of yak CL, respectively. On the contrary, two miRNAs exhibited varied expression across the CL cycle. bta-miR-30f, was found to be highly expressed in the early stage, while bta-miR-26a, was highly expressed in the subsequent two stages.

Base performance analysis

The base distribution characteristics of miRNAs between 18 and 25 nt were analyzed. For both known and novel miRNA, more than half of the base sites displayed uracil (U) preference (Fig. 2A and B). miRNAs are reported to display a strong preference for U at the 5′-end.[37] Here we found that both the known and novel miRNAs with the length between 19 and 25 nt displayed U preference at the first base site, while known and novel miRNAs with the length of 18 nt exhibited adenine (A) and cytosine (C) preference at their 5′-ends, respectively (Fig. 2C and D).

Differentially expressed miRNAs in yak CL of three stages

To identify the potential roles of miRNAs in yak CL, differentially expressed (DE) miRNAs during the estrous cycle were investigated. A total of 1,067, 280, and 112 DE miRNAs were found in eCL vs. mCL, mCL vs. lCL and eCL vs. lCL, respectively (Table S4). The expression patterns of all DE miRNAs were displayed in volcano plots (Fig. 3A–C) and hierarchical clustering map (Fig. 3D). Most DE miRNAs were
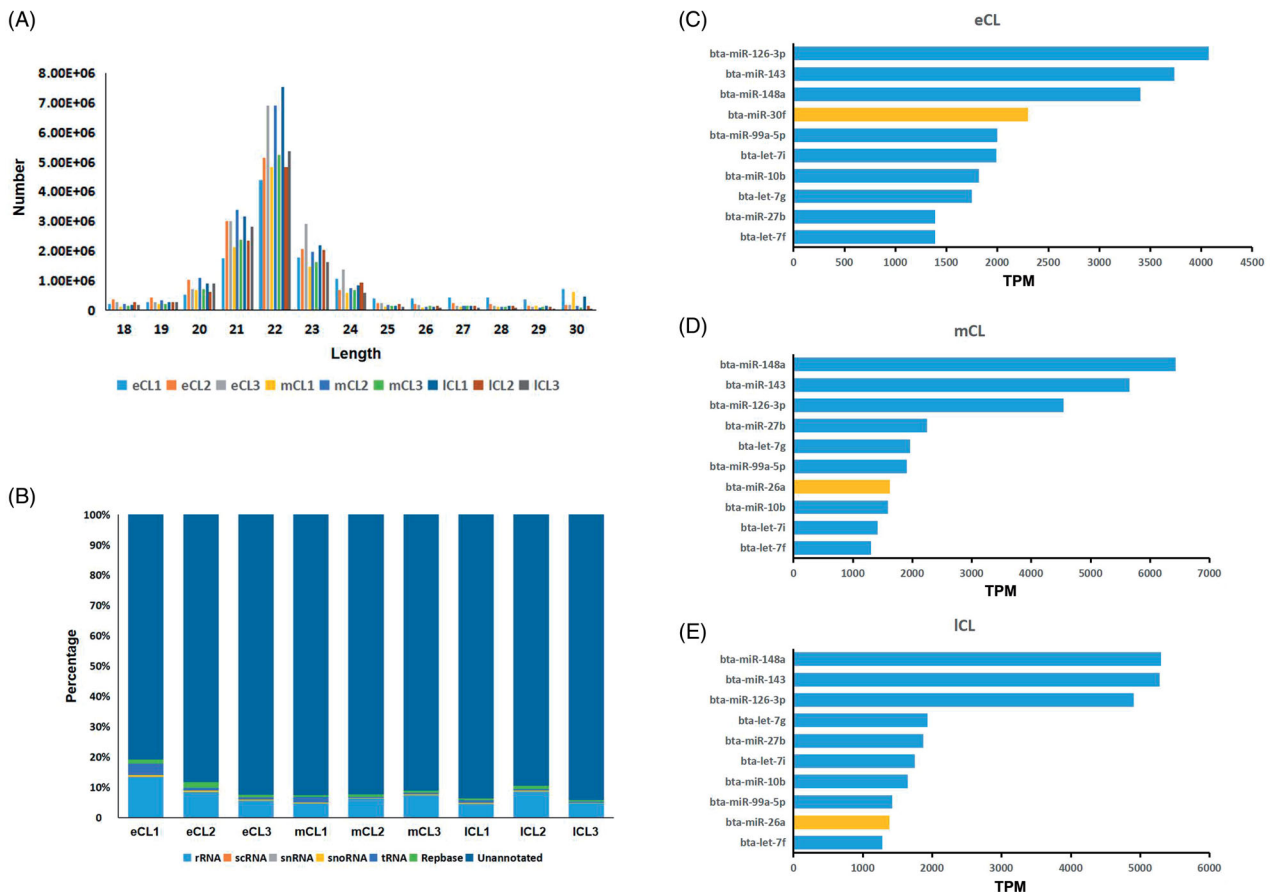
Figure 1. Identification of miRNAs in yak CLs at different stages. (A) Annotation classification of small RNAs (sRNAs). The proportion of ribosomal RNA (rRNA), transport RNA (tRNA), nuclear small RNA (snRNA), nucleolar small RNA (snoRNA), repeated sequences (Rebase) and unannotated RNA (Unannotated) are labeled with different colors, as mentioned in the bottom of the figure. (B) The length distribution of clean reads in different samples. eCL1 to eCL3, mCL1 to mCL2 and lCL1 to lCL3 represented three replicate CL samples in early, middle and late stages, respectively. The same as below. (C–E) The top ten most abundant miRNAs at each stage of yak CL. The miRNAs represented by blue bars are highly expressed at each stage. The miRNAs represented by orange bars are only highly expressed in only one of the three stages.

down-regulated in eCL vs. mCL (781 of 1,067) and eCL vs. lCL (88 of 112). While in mCL vs. lCL group, 268 DE miRNAs were up-regulated and only 12 were down-regulated (Table S4). We listed the top ten DE miRNAs with the most significant changes in each group (Fig. 3F–G) and found that most of the miRNAs were down-regulated in the eCL vs. mCL group (nine of ten) and eCL vs. lCL group (nine of ten). In contrast, eight miRNAs were up-regulated while only two were down-regulated in the mCL vs. lCL group. Among these DE miRNAs, novel-miR-794 and bta-miR-1246 were down-regulated in both eCL vs. mCL group and eCL vs. lCL group. Another two miRNAs, bta-miR-96 and bta-miR-183, displayed dramatic decreased expressions from the eCL to mCL stage, and then a significant increasing trend from the mCL to lCL stage (Fig. 3F–G).

To validate the expression profiles of DE miRNAs, six DE miRNAs with different expression trends,

including bta-miR-101, bta-miR-432, bta-miR-451, bta-miR-6522, novel-miR-98, and novel-miR-701, were selected and their expressions were detected by real-time PCR. Consistent expression trends from both real-time PCR and miRNA-seq for all the selected miRNAs confirmed the reliability of sequencing data (Table 2).

Function analyses of DE miRNAs target genes

DE miRNAs target genes were predicted by miRanda (version:v3.3a) and Targetscan (version:6.0). A total of 18,904 target genes were identified, and 18,843 were annotated from NR, Swiss-Prot, COG, KEGG, KOG or Pfam database (Table S5). The numbers of annotated target genes for DE miRNAs in eCL vs. mCL, eCL vs. lCL, and mCL vs. lCL were 13,003, 9,280, and 7,937, respectively. KEGG (Kyoto Encyclopedia of Genes and Genomes) database is an important public database used to analyses of gene enrichment.[38] The DE
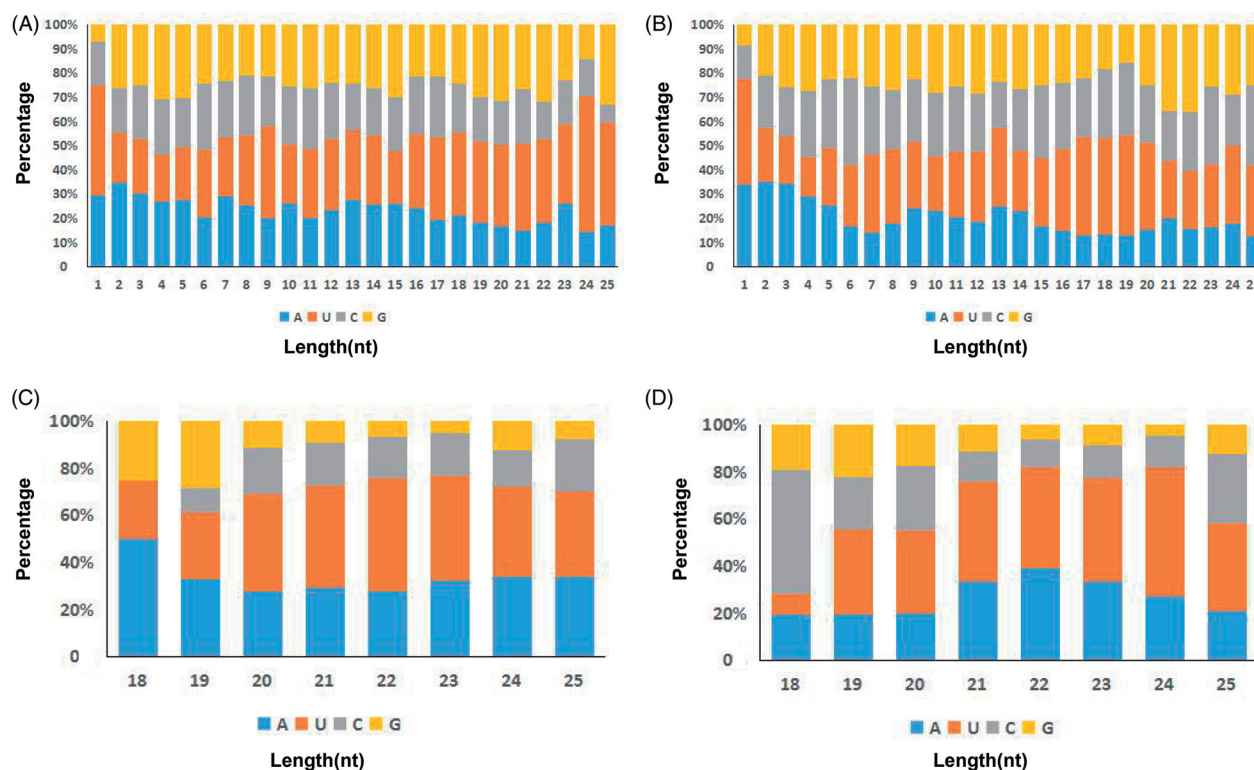
Figure 2. The base distribution characteristics of miRNAs between 18 and 25 nt in length in yak CLs. (A–B) Base performance for each site of known (A) and novel (B) miRNAs. (C–D) Base performance of the first site of known (C) and novel miRNAs (D). The proportions of Adenine (A), Uracil (U), Guanine (G) and Cytosine (C) are labeled with different colors as mentioned in the bottom of the figure.

miRNAs target genes were classified based on the types of cellular KEGG pathways (Table S6). The top ten pathways enrichment of genes targeted by at least three DE miRNAs in each group were displayed and the top three pathway included pathways in cancer (ko05200), PI3K-Akt pathway (ko04151), endocytosis (ko04144), and focal adhesion (ko04510) (Fig. 4).

Identification of DE miRNA target genes related to yak CL

A total of 20 target genes for 47 DE miRNAs were found to be associated with the development, function or regression of CL (Table 3). These genes were divided into three groups: ten genes were associated with CL development through the regulation of cell proliferation (cyclin-dependent kinase 2 (CDK2) and CDK4), GC luteinization (class II major histocompatibility complex (MHC-II) and dipeptidyl peptidase 4 (DPP4)), endothelial cell migration (sphingosine-1-phosphate receptor 1 (S1PR1), S1PR3 and S1PR5), vasculogenesis (S1PR5 and vasohibin-1(VASH1)), and ECM remodeling (bone morphogenetic protein 2 (BMP2). Six genes were involved in progesterone production, including M1R,

scavenger receptor class B member 1 (SR-BI), estradiol 17-beta-dehydrogenase 1 (HSD17B1), hydroxysteroid 11-beta dehydrogenase 2 (HSD11B2), glucocorticoid receptor (GR), and peroxisome proliferator-activated receptor delta (PPARD), and six genes were related to CL regression by regulating apoptosis (caspase 2 (CASP2), BCL2 like 1 (BCL2L1)), autophagy (autophagy related 3 (ATG3) and microtubule associated protein 1 light chain 3 gamma (MAP1LC3C)), blocking steroidogenesis (heat shock protein family A member 1B (HSP701B)), and regulating cell sensitivity to cytokines (suppressors of cytokine signaling 3 (SOCS-3)).

Luciferase assay was performed to determine whether three DE miRNAs, including bta-miR-11972, novel-miR-619 and novel-miR-153, can directly bind to the 3′-UTR of their putative target mRNAs. The 293 T cell that transfected with vectors containing the 3′-UTR of CDK4 mRNA and bta-miR-11972 mimics exhibited a significant decrease in luciferase activity. By contrast, no significant change was found in cells co-transfected with the blank constructs and bta-miR-11972 mimics. Similarly, novel-miR-619 and novel-miR-153 were also proved to directly bind to the 3′-UTR region of their target mRNAs (Fig. 5).
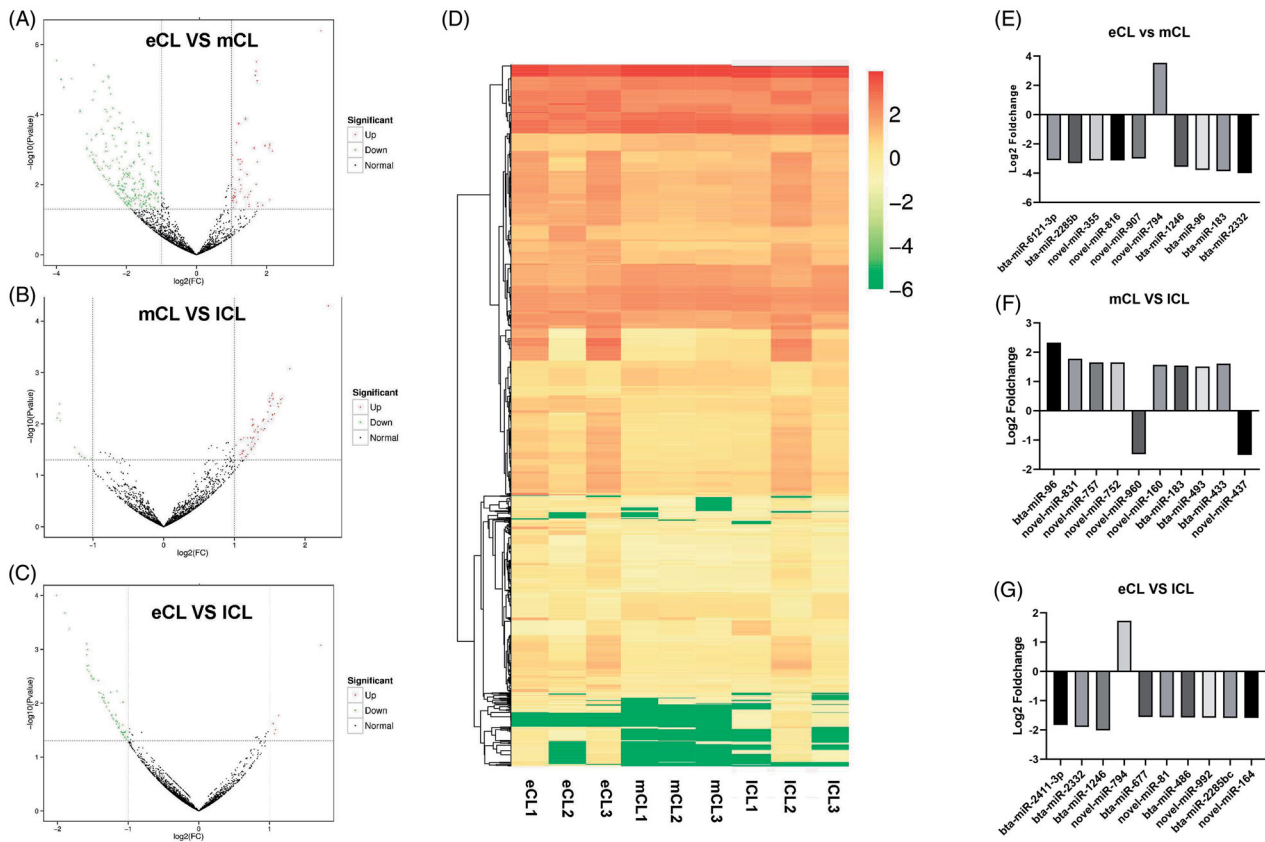
Figure 3. DE miRNAs in yak CL in the three stages. (A–C) Volcano plot of all miRNAs among eCL vs mCL (A), mCL vs lCL (B) and eCL vs lCL (C). The Y-axis represents the negative logarithm value of the error detection rate. Blue dots represent miRNAs without differential expression, red dots represent significantly up-regulated miRNAs, and green dots represent significantly down-regulated miRNAs. (D) The heatmap of the miRNAs in the three stages of yak CL. Columns represent different samples and rows represent different miRNAs. The clustering is based on lg (TPM + 1e-6) value. Red indicates miRNAs with high expression and green indicates miRNAs with low expression. (E–G) The top ten DE miRNAs with the most significant changes in eCL vs. mCL (E), mCL vs. lCL (F) and eCL vs. lCL (G) groups.

Table 2. Expression profiles of six DE miRNAs which were randomly selected for the validation of miRNA-seq.

	eCL vs. mCL				mCL vs. lCL				eCL vs. lCL			
	Fold-change		p-Value		Fold-change		p-Value		Fold-change		p-Value	
miRNA- ID	mSeq	qPCR	mSeq	qPCR	mSeq	qPCR	mSeq	qPCR	mSeq	qPCR	mSeq	qPCR
bta-miR-451	1.74	4.62	>0.05	0.0588	1.68	4.21	>0.05	0.8159	**2.93**	**19.5**	**0.00963**	**0.0278**
bta-miR-6522	**0.318**	**0.541**	**0.00223**	**0.0256**	1.513	1.54	>0.05	0.0718	**0.481**	**0.833**	>0.05	0.688
bta-miR-432	**9.82**	**3.79**	**8.76E-06**	**0.0061**	**0.288**	**0.844**	**0.0087**	**0.9430**	2.83	3.20	>0.05	0.860
bta-miR-101	**0.353**	**0.137**	**3.11E-06**	**0.0232**	1.47	1.75	>0.05	0.2357	0.518	0.239	>0.05	0.2267
novel-miR-701	**0.211**	**0.192**	**0.0419**	**0.0001**	**5.27**	**5.87**	**0.0390**	**0.0001**	1.11	1.128	>0.05	0.9290
novel-miR-98	**3.77**	**2.741**	**0.000325**	**0.0090**	0.797	1.151	>0.05	0.9371	**3.01**	**3.16**	**0.00598**	**0.0063**

mSeq: miRNA-Seq, qPCR: Real-time PCR.
The real-time PCR fold change was calculated using the comparative C_T method and miRNA levels were normalized and plotted against *U6*. Significance between different classes was assessed by one-way ANOVA (Tukey's multiple comparison test). Significant regulation ($p < 0.05$) was indicated in bold.

Expression profiles of these DE miRNAs and their target mRNAs in different stages of yak CLs were further analyzed. The expression of bta-miR-11972 increased significantly from eCL to mCL then decreased dramatically. *CDK4* is the target gene of miR-bta-11972 and its expression decreased slightly from eCL to mCL stage and then increased significantly. novel-miR-153 displayed a similar expression profile to bta-miR-11972. The expression of its target gene, *HSD17B1*, was up-regulated from eCL to mCL, and then decreased in lCL stage. Another DE miRNA, novel-miR-619, was highly expressed in the eCL stage and displayed a sharp decrease in the mCL stage, followed by a significant increase in the lCL stage. Its target gene, *MAP1LC3C*, exhibited a persistent increase from the eCL to lCL stage (Fig. 6, Table S7).
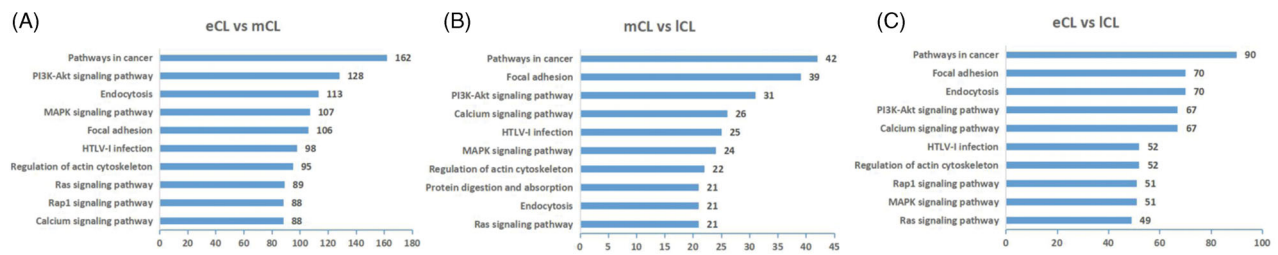
Figure 4. KEGG pathways enrichment of genes targeted by at least three DE miRNAs in either: eCL vs. mCL, mCL vs. lCL, or eCL vs. lCL(A-C). The top ten most significantly enriched pathways in each group. The Y-axis represents the name of different KEGG pathways. Numbers behind each column represent the number of target genes annotated in the corresponding pathways.

Table 3. DE miRNAs and their target genes involved in CL development.

| Gene	DE miRNAs	Functional category
CDK2	bta-miR-1291; novel-miR-316; novel-miR-712;; novel-miR-869	Luteal cell proliferation
CDK4	bta-miR-11972	Luteal cell proliferation
MHC-II	novel-miR-258; novel-miR-759; novel-miR-608	GC luteinization
DPP4	bta-miR-10182-3p; novel-miR-157; novel-miR-225; novel-miR-390; novel-miR-619; novel-miR-757; novel-miR-794; novel-miR-882	GC luteinization
VASH1	novel-miR-62; novel-miR-241; novel-miR-455; novel-miR-779; novel-miR-889	Vasculogenesis
S1PR1	bta-miR-11972	Endothelial cell migration
S1PR3	bta-miR-432; novel-miR-619; novel-miR-906	Endothelial cell migration
S1PR5	bta-miR-10182-5p; novel-miR-619; novel-miR-944	Vasculogenesis; endothelial cell migration
BMP2	bta-miR-370; bta-miR-2403; bta-miR-10182-3p; novel-miR-390; novel-miR-960	ECM remolding
SR-BI	bta-miR-874; novel-miR-691; novel-miR-757	Steroidogenesis
HSD17B1	bta-miR-3956; novel-miR-157; novel-miR-455; novel-miR-619; novel-miR-712; novel-miR-816	Steroidogenesis
HSD11B2	novel-miR-437; bta-miR-24-3p	Steroidogenesis
GR	bta-miR-184; novel-miR-265	Steroidogenesis
PPARD	bta-miR-11972; bta-miR-432; novel-miR-241; novel-miR-130; novel-miR-157; novel-miR-710	Steroidogenesis
CASP2	bta-miR-2431-3p; novel-miR-229; novel-miR-535	CL regression (Pro-apoptosis)
BCL2L1	bta-miR-11978; novel-miR-18; novel-miR-62; novel-miR-619; novel-miR-751; novel-miR-759	CL regression (Anti-apoptosis)
ATG3	bta-miR-11978; novel-miR-779	CL regression (Autophagy)
MAP1LC3C	novel-miR-153	CL regression (Autophagy)
HSP701B	bta-miR-874; bta-miR-11978; novel-miR-316	CL regression (Blocking Steroidogenesis)
SOCS-3	bta-miR-432; novel-miR-992; novel-miR-130 novel-miR-225	CL regression (Decreasing cell sensitivity to cytokines)
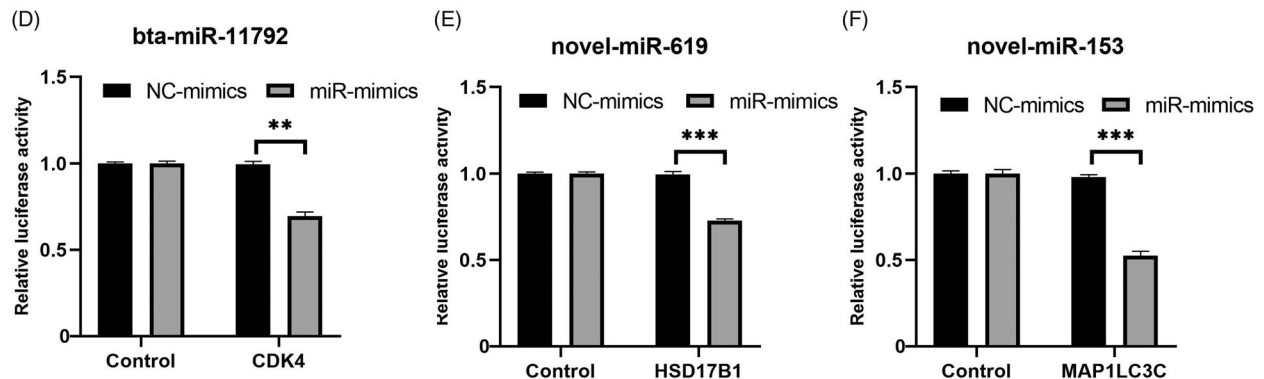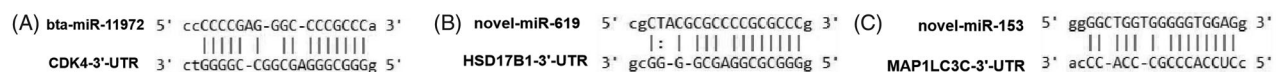
Figure 5. bta-miR-11972, novel-miR-619 and novel-miR-153 directly bind to the 3′-UTR of their putative target mRNAs. (A–C) Sequence alignment of bta-miR-11972, novel-miR-619 and novel-miR-153-binding sites in the 3′-UTR of their putative target mRNAs CDK4 (A), HSD17B1 (B) and MAP1LC3C (C). (D–F) Relative luciferase activities of blank vectors (control) or vectors carrying 3′-UTRs of target mRNAs in 293 T cells co-transfected with miRNA mimics (miR-mimics) or negative control mimics (NC-mimics).
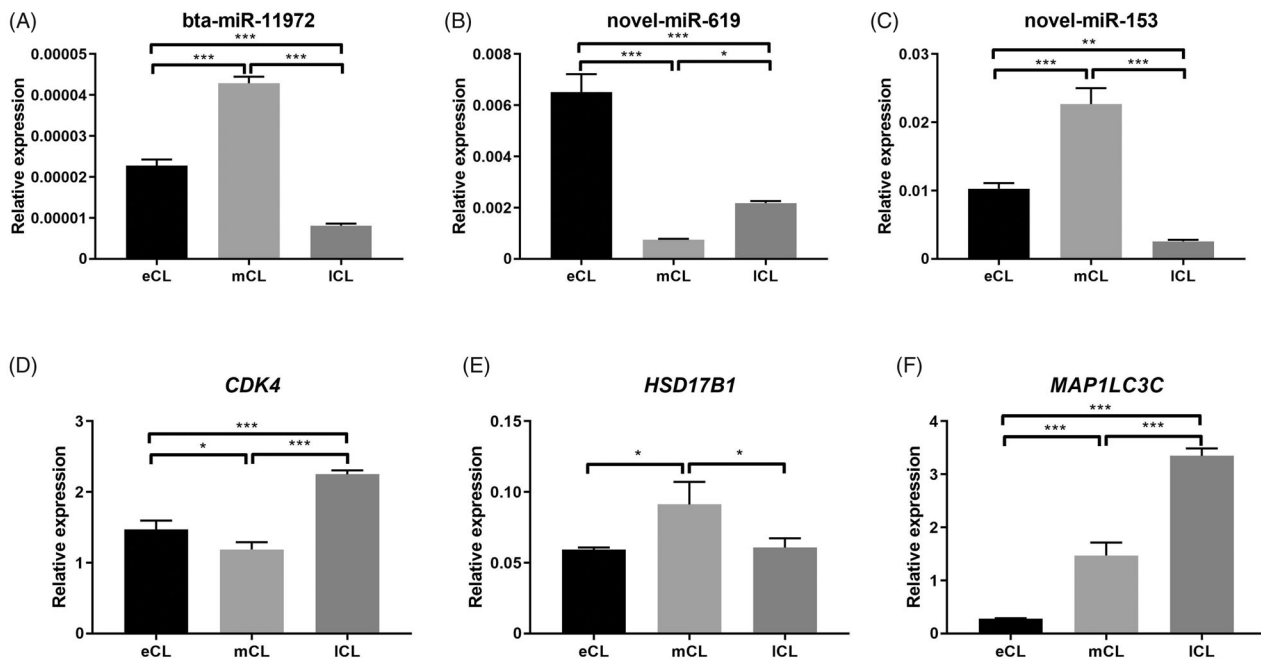
Figure 6. Expression detection of several DE miRNAs and their target genes that are related to CL development. (A–C). Expression levels of three DE miRNAs, bta-miR-11972, novel-miR-619 and novel-miR-153. The miRNA levels were normalized and plotted against *U6*. $*p < 0.05$, $**p < 0.01$, and $***p < 0.001$, one-way ANOVA (Tukey's multiple comparison test). Data shown are expressed as mean ± SEM from three independent experiments. (D–F) Expression detection of target genes, including *CDK4* (the target gene of bta-miR-11972), *HSD17B1* (novel-miR-619) and *MAP1LC3C* (novel-miR-153). mRNA levels were normalized and plotted against *SUZ12*. $*p < 0.05$, $**p < 0.01$, and $***p < 0.001$, one-way ANOVA (Tukey's multiple comparison test). Data shown are expressed as mean ± SEM from three independent experiments.

Discussion

Corpus luteum is a transient endocrine organ in female animals and is essential for regulating the length of the estrous cycle.[2,3,39] Recently numerous studies have characterized that miRNAs involved in CL development in different domestic animals, such as buffalo and bovine.[20,21] However, little is known about the miRNA transcriptome in yak CL. In this study, we analyzed the miRNA profiles in different stages of yak CLs. Besides, we identified DE miRNAs and their predicted target genes via *in-silico* simulations during yak CL development, maintenance and regression. The findings provide valuable information for future studies on the regulation of miRNA on yak CL. To our knowledge, this study for the first time identifies and analyzes miRNAs in yak CL.

Analysis of the top ten most abundant miRNAs in yak CLs revealed that nine miRNAs, including bta-miR-126-3p, bta-miR-143, bta-miR-148a, bta-miR-99a-55p, bta-let-7i, bta-miR-10b, bta-let-7g, bta-miR-27b and bta-let-7f constantly exhibited abundant expressions across the estrous cycle. Interestingly, all the nine miRNAs were also highly expressed across the lifespan of bovine CL, except for bta-miR-126-3p.[21] bta-miR-126-3p was identified as one of the top three, most abundant miRNAs in each stage of yak CL, however, it was absent in the top twenty most abundantly sequenced miRNAs in the bovine CL. Another study reported that the expression of bta-miR-126-3p in bovine CL was significantly more abundant in mCL and lCL, than in the early stages,[40] while our result showed that this miRNA was constantly highly expressed across the entire yak CL lifespan and didn't exhibit a dynamic expression trend (Table S3). In future studies, the focus should be on identifying the putative involvement of bta-miR-126-3p in the development of both bovine and yak CL.

Most of the miRNAs in yak CLs displayed U preference at the 5′-end, except for miRNAs with a length of 18 nt (Fig. 2C and D). The 18 nt known and novel miRNAs showed A and C preference at the 5′-ends (Fig. 2C and D). The different preference of the first base of miRNA with different lengths were also founded in other tissues. In the bovine brains, miRNAs with a length of 25 nt exhibited A preference,[41] while in goats rumens miRNAs which are 18 nt in length displayed A and G preferences.[42] Studies have reported that the differences in base content at the 5′-end might be associated with the switch in miRNA silencing mechanisms in some species,[43] while further studies are

needed to elucidate the biological significance of first base preference of miRNA in yak CLs.

A total of 1067, 280, and 112 DE miRNAs were identified in the eCL vs. mCL, mCL vs. lCL, and eCL vs. lCL group, respectively (Table S5). As shown, more than 70% of the DE miRNAs were found during the transition from eCL to mCL. Besides, among the 47 DE miRNAs related to CL development, 38 miRNAs were differentially expressed in the eCL vs. mCL group. In the 20 DE miRNA target genes, 14 genes were associated with CL formation or progesterone synthesis and they mainly functioned in early or middle CL stage. These results implied that the stage from eCL to mCL might be an ideal period for studying the regulation of miRNA in yak CL.

Among the top ten DE miRNAs with the most significant changes, bta-miR-96 was highly expressed in eCL, and then decreased consistently. Interestingly, this miRNA also exhibited a dynamic expression profile in bovine CLs. bta-miR-96 was significantly up-regulated in bovine eCL, followed by a significant down-regulation in later stages.[21] A study on human luteinized granulosa cells showed that miR-96 acts as a negative regulator of steroidogenesis by repressing the expression of forkhead box O1 (*Foxo1*) . However, although this miRNA is highly conserved among different species, its inhibition of progesterone production has not been observed in bovine luteal cells.[44] Considering the close relationship between yak and bovine, whether bta-miR-96 can regulate progesterone production is not clear.

In this study, we found that DE miRNAs target genes in yak CLs were involved in various biological processes, including cell proliferation, GC luteinization, endothelial cell migration, vasculogenesis, ECM remodeling, steroidogenesis, cellular apoptosis and autophagy.[45–52] Luciferase assay verified that three of them, including *CDK4*, *HSD17B1*, and *MAP1LC3C*, were directly targeted by bta-miR-11972, novel-miR-619 and novel-miR-153, respectively (Fig. 5). In addition, we found two target genes, *CDK4* and *HSD17B1*, displayed opposite expression tendencies with the DE miRNAs which targeting them (bta-miR-11972 and novel-miR-153) across the entire lifespan of yak CL. *CDK4* encodes a cyclin-dependent kinase and is responsible for regulating cell cycle progression.[53] HSD17B1 catalyzes the conversion of low active 17-ketosteroids, androstenedione and estrone to highly active 17-hydroxysteroids.[54] Another autophagy-related gene, *MAP1LC3C*, displayed the opposite tendency with the miRNA targeting it only during the transition from mCL to lCL (Fig. 5). The relationships between these DE miRNAs and their target genes may give new inspirations to explore the potential roles of miRNA in the formation, functionalization and regression of yak CL in the future.

Disclosure statement

No potential conflict of interest was reported by the author(s).

Funding

ORCID

Shi Yin http://orcid.org/0000-0001-7730-633X

Data availability statement

The raw data have been deposited in the NCBI Sequence Read Archive (SRA) database with the accession number SRR13108178-SRR13108186.

References

1. Bachelot A, Binart N. Corpus luteum development: lessons from genetic models in mice. *Curr Top Dev Biol*. 2005;68:49–84.
2. Kfir S, Basavaraja R, Wigoda N, Ben-Dor S, Orr I, Meidan R. Genomic profiling of bovine corpus luteum maturation. *PLOS One*. 2018;13(3):e0194456.
3. Smith MF, McIntush EW, Smith GW. Mechanisms associated with corpus luteum development. *J Anim Sci*. 1994;72(7):1857–1872.
4. Devoto L, Kohen P, Munoz A, Strauss JF. 3rd. Human corpus luteum physiology and the luteal-phase dysfunction associated with ovarian stimulation. *Reprod Biomed Online*. 2009;18(Suppl 2):19–24.
5. Devoto L, Henriquez S, Kohen P, Strauss JF. 3rd. The significance of estradiol metabolites in human corpus luteum physiology. *Steroids*. 2017;123:50–54.
6. Wuttke W, Theiling K, Hinney B, Pitzel L. Regulation of steroid production and its function within the corpus luteum. *Steroids*. 1998;63(5–6):299–305.
7. Skarzynski DJ, Ferreira-Dias G, Okuda K. Regulation of luteal function and corpus luteum regression in cows: hormonal control, immune mechanisms and intercellular communication. *Reprod Domest Anim*. 2008;43 Suppl 2:57–65.
8. Niswender GD, Juengel JL, Silva PJ, Rollyson MK, McIntush EW. Mechanisms controlling the function and life span of the corpus luteum. *Physiol Rev*. 2000; 80(1):1–29.
9. Ziecik AJ, Przygrodzka E, Jalali BM, Kaczmarek MM. Regulation of the porcine corpus luteum during pregnancy. *Reproduction*. 2018;156(3):R57–R67.

10. Magata F, Shirasuna K, Struve K, et al. Gene expressions in the persistent corpus luteum of postpartum dairy cows: distinct profiles from the corpora lutea of the estrous cycle and pregnancy. *J Reprod Dev*. 2012; 58(4):445–452.

11. Stocco C, Telleria C, Gibori G. The molecular control of corpus luteum formation, function, and regression. *Endocr Rev*. 2007;28(1):117–149.

12. Curlewis JD, Tam SP, Lau P, et al. A prostaglandin f(2alpha) analog induces suppressors of cytokine signaling-3 expression in the corpus luteum of the pregnant rat: a potential new mechanism in luteolysis. *Endocrinology*. 2002;143(10):3984–3993.

13. Choi J, Jo M, Lee E, Choi D. The role of autophagy in corpus luteum regression in the rat. *Biol Reprod*. 2011;85(3):465–472.

14. Jiang YF, Hsu MC, Cheng CH, Tsui KH, Chiu CH. Ultrastructural changes of goat corpus luteum during the estrous cycle. *Anim Reprod Sci*. 2016;170:38–50.

15. Vishnoi A, Rani S. MiRNA biogenesis and regulation of diseases: an overview. *Methods Mol Biol*. 2017;1509: 1–10.

16. Cai Y, Yu X, Hu S, Yu J. A brief review on the mechanisms of miRNA regulation. *Genomics Proteomics Bioinformatics*. 2009;7(4):147–154.

17. Hausser J, Syed AP, Bilen B, Zavolan M. Analysis of CDS-located miRNA target sites suggests that they can effectively inhibit translation. *Genome Res*. 2013; 23(4):604–615.

18. Ivashchenko A, Berillo O, Pyrkova A, Niyazova R. Binding sites of miR-1273 family on the mRNA of target genes. *Biomed Res Int*. 2014;2014:620530.

19. Otsuka M, Zheng M, Hayashi M, et al. Impaired microRNA processing causes corpus luteum insufficiency and infertility in mice. *J Clin Invest*. 2008; 118(5):1944–1954.

20. Jerome A, Thirumaran SMK, Kala SN. Identification of microRNAs in corpus luteum of pregnancy in buffalo (*Bubalus bubalis*) by deep sequencing. *Iran J Vet Res*. 2017;18(4):287–290.

21. Gecaj RM, Schanzenbach CI, Kirchner B, et al. The dynamics of microRNA transcriptome in bovine corpus luteum during its formation, function, and regression. *Front Genet*. 2017;8:213.

22. Maalouf SW, Liu WS, Albert I, Pate JL. Regulating life or death: potential role of microRNA in rescue of the corpus luteum. *Mol Cell Endocrinol*. 2014; 398(1–2):78–88.

23. Maalouf SW, Smith CL, Pate JL. Changes in microRNA expression during maturation of the bovine corpus luteum: regulation of luteal cell proliferation and function by microRNA-34a. *Biol Reprod*. 2016;94(3):71.

24. Xu MQ, Jiang H, Zhang LQ, et al. MiR-29b affects the secretion of PROG and promotes the proliferation of bovine corpus luteum cells. *PLOS One*. 2018;13(4): e0195562.

25. Farberov S, Meidan R. Fibroblast growth factor-2 and transforming growth factor-beta1 oppositely regulate miR-221 that targets thrombospondin-1 in bovine luteal endothelial cells. *Biol Reprod*. 2018;98(3): 366–375.

26. Prakash BS, Sarkar M, Mondal M. An update on reproduction in yak and mithun. *Reprod Domest Anim*. 2008;43 Suppl 2:217–223.

27. Lan D, Xiong X, Huang C, Mipam TD, Li J. Toward understanding the genetic basis of yak ovary reproduction: a characterization and comparative analyses of estrus ovary transcriptiome in yak and cattle. *PLOS One*. 2016;11(4):e0152675.

28. Zhang Q, Wang Q, Zhang Y, et al. Comprehensive analysis of microRNA(–)messenger RNA from white yak testis reveals the differentially expressed molecules involved in development and reproduction. *Int J Mol Sci*. 2018;19(10):3083.

29. Zhao W, Quansah E, Yuan M, et al. Next-generation sequencing analysis reveals segmental patterns of microRNA expression in yak epididymis. *Reprod Fertil Dev*. 2020;32(12):1067–1083.

30. Xie J, Kalwar Q, Yan P, Guo X. Effect of concentrate supplementation on the expression profile of miRNA in the ovaries of yak during non-breeding season. *Animals*. 2020;10(9):1640.

31. Yao Y, Niu J, Sizhu S, et al. microRNA-125b regulates apoptosis by targeting bone morphogenetic protein receptor 1B in yak granulosa cells. *DNA Cell Biol*. 2018;37(11):878–887.

32. Berisha B, Schams D, Rodler D, Sinowatz F, Pfaffl MW. Expression and localization of members of the thrombospondin family during final follicle maturation and corpus luteum formation and function in the bovine ovary. *J Reprod Dev*. 2016;62(5):501–510.

33. Berisha B, Schams D, Rodler D, Sinowatz F, Pfaffl MW. Expression pattern of HIF1alpha and vasohibins during follicle maturation and corpus luteum function in the bovine ovary. *Reprod Dom Anim*. 2017;52(1): 130–139.

34. Rekawiecki R, Rutkowska J, Kotwica J. Identification of optimal housekeeping genes for examination of gene expression in bovine corpus luteum. *Reprod Biol*. 2012;12(4):362–367.

35. Gallego Romero I, Pai AA, Tung J, Gilad Y. RNA-seq: impact of RNA degradation on transcript quantification. *BMC Biol*. 2014;12:42.

36. Ewing B, Hillier L, Wendl MC, Green P. Base-calling of automated sequencer traces using phred. I. Accuracy assessment. *Genome Res*. 1998;8(3):175–185.

37. Liu X, Jin DY, McManus MT, Mourelatos Z. Precursor microRNA-programmed silencing complex assembly pathways in mammals. *Mol Cell*. 2012;46(4): 507–517.

38. Altermann E, Klaenhammer TR. PathwayVoyager: pathway mapping using the Kyoto encyclopedia of genes and genomes (KEGG) database. *BMC Genomics*. 2005;6:60.

39. Reynolds LP, Redmer DA. Growth and development of the corpus luteum. *J Reprod Fertil Suppl*. 1999;54: 181–191.

40. Dai L, Xu J, Liu S, et al. Characterization of miR-126-3p and its target talin2 in the bovine corpus luteum during the oestrus cycle. *Reprod Dom Anim*. 2014; 49(6):913–919.

41. Jin W, Grant JR, Stothard P, Moore SS, Guan LL. Characterization of bovine miRNAs by sequencing and bioinformatics analysis. *BMC Mol Biol.* 2009;10:90.

42. Zhong T, Hu J, Xiao P, et al. Identification and characterization of microRNAs in the goat (*Capra hircus*) rumen during embryonic development. *Front Genet.* 2017;8:163.

43. Shi B, Gao W, Wang J. Sequence fingerprints of microRNA conservation. *PLOS One.* 2012;7(10): e48256.

44. Mohammed BT, Sontakke SD, Ioannidis J, Duncan WC, Donadeu FX. The adequate corpus luteum: miR-96 promotes luteal cell survival and progesterone production. *J Clin Endocrinol Metab.* 2017;102(7): 2188–2198.

45. Becker S, von Otte S, Robenek H, Diedrich K, Nofer JR. Follicular fluid high-density lipoprotein-associated sphingosine 1-phosphate (S1P) promotes human granulosa lutein cell migration via S1P receptor type 3 and small G-protein RAC1. *Biol Reprod.* 2011;84(3): 604–612.

46. Donadeu FX, Sanchez JM, Mohammed BT, et al. Relationships between size, steroidogenesis and miRNA expression of the bovine corpus luteum. *Theriogenology.* 2020;145:226–230.

47. Grzesiak M, Michalik A, Rak A, Knapczyk-Stwora K, Pieczonka A. The expression of autophagy-related proteins within the corpus luteum lifespan in pigs. *Domest Anim Endocrinol.* 2018;64:9–16.

48. Hampl A, Pachernik J, Dvorak P. Levels and interactions of p27, cyclin D3, and CDK4 during the formation and maintenance of the corpus luteum in mice. *Biol Reprod.* 2000;62(5):1393–1401.

49. Hoffmann B, Busges F, Baumgartner W. Immunohistochemical detection of CD4-, CD8- and MHC II-expressing immune cells and endoglin in the canine corpus luteum at different stages of dioestrus. *Reprod Domest Anim.* 2004;39(6):391–395.

50. Shirasuna K, Kobayashi A, Nitta A, et al. Possible action of vasohibin-1 as an inhibitor in the regulation of vascularization of the bovine corpus luteum. *Reproduction.* 2012;143(4):491–500.

51. Wu L, Feng J, Mu Y, et al. O45-regulation of osteoblast differentiation and ECM remodeling by Bmp2/4 *in vitro. Bull Group Int Rech Sci Stomatol Odontol.* 2011;49(3):94–97.

52. Zorrilla LM, D'Annibale MA, Swing SE, Gadsby JE. Expression of genes associated with apoptosis in the porcine corpus luteum during the oestrous cycle. *Reprod Domest Anim.* 2013;48(5):755–761.

53. Tsutsui T, Hesabi B, Moons DS, et al. Targeted disruption of CDK4 delays cell cycle entry with enhanced p27(Kip1) activity. *Mol Cell Biol.* 1999; 19(10):7011–7019.

54. Hakkarainen J, Jokela H, Pakarinen P, et al. Hydroxysteroid (17β)-dehydrogenase 1-deficient female mice present with normal puberty onset but are severely subfertile due to a defect in luteinization and progesterone production. *Faseb J.* 2015;29(9): 3806–3816.